

Robust Timing Synchronization Preamble for MIMO-OFDM Systems Using Mapped CAZAC Sequences

Ali Rachini

Fabienne Nouvel

Ali Beydoun and Bilal Beydoun

IETR - INSA de Rennes, France

GET/UL - Lebanese University

Email: Ali.Rachini@ul.edu.lb fabienne.nouvel@insa-rennes.fr

IETR - INSA de Rennes

Rennes, France

GET/UL - Lebanese University

Hadath, Lebanon

bilbey@ul.edu.lb

beydoul@yahoo.fr

Abstract—Orthogonal frequency division multiplexing system provides a promising physical layer for 4G and 3GPP LTE systems in terms of efficient use of bandwidth and high data rates, this technology suffers from Inter Symbol Interference and Inter Carrier Interference. On the other hand, multiple input - multiple output system is deployed along with orthogonal frequency division multiplexing in the new 802.11n standard, which offers many advantages over conventional standards such as 802.11g Wireless LAN. The main challenge of such system is the synchronization between the transmitter and the receiver [1]. A bad timing synchronization causes the loss of a lot of information in a MIMO-OFDM system. In this paper, a robust timing synchronization method is proposed for a MIMO-OFDM systems up to 8×8 as well, where N_t is the transmit antennas and N_r is the receive antennas. The proposed method is based on transmit a mapped orthogonal constant amplitude zero auto correlation sequences over different transmit antennas. The simulations results show that the proposed method has high performance to detect the timing synchronization even at very low signal to noise ratio in additive white Gaussian noise and multipath fading Rayleigh channels. Furthermore, simulation results for our proposed method present a robust timing synchronization against existing methods at a low SNR and for MIMO-OFDM system up to 8×8 , which the coarse and fine timing synchronization are done at the same time at each receive antenna due to the orthogonality of different training sequences transmitted over different transmit antennas.

Keywords - MIMO-OFDM system; fine timing synchronization; coarse timing synchronization; CAZAC sequences; compact preamble.

I. INTRODUCTION

The wireless-communications revolution grows continuously in order to increase throughput, which can only be achieved through the development of new communication technologies. In this context, different wireless communication technologies offer enormous increase of channel capacity like Multiple Input Multiple Output - Orthogonal Frequency Division Multiplexing (MIMO-OFDM) systems. Therefore, the combination between MIMO and OFDM systems is proposed in 802.11n [2].

The OFDM [3] is a digital Multi-carrier modulation technology in which a large number of closely spaced orthogonal subcarriers are used to carry the data. OFDM

became a very popular multi-carrier modulation technique for transmission of signals over wireless channels. OFDM has been deployed in many applications like IEEE 802.11a, HIPERLAN/2 wireless LANs, Digital Video Broadcasting, and satellite radio.

It divides the data into several orthogonal and parallel data streams (N_{sc}) called sub-carrier or sub-channel. Each sub-carrier is modulated with a conventional modulation such as M-ary schemes like Phase Shift Keying (M-PSK) or Quadrature Amplitude Modulation (QAM), also, the total data rate is maintained similar to those in a conventional single-carrier modulation scheme in the same bandwidth. To maintain the orthogonality, the space required between two consecutive sub-carriers is $\Delta f = \frac{1}{T_s}$, where T_s is the duration of OFDM symbol.

The implementation of OFDM systems is very easy, on the other hand, the OFDM modulator/demodulator can be done by a simple Inverse Fast Fourier Transform (IFFT) and Fast Fourier Transform (FFT) algorithm [4], respectively. The main drawback of OFDM technology is high Peak-to-Average Power ratio (PAPR), which means randomly sinusoidal leads occurred during transmission of the OFDM signal.

Otherwise, OFDM technology suffers from Inter Symbol Interference (ISI) and Inter Carrier Interference (ICI). OFDM uses Cyclic Prefix (CP) or Guard Interval (GI) in order to combat the ISI and ICI introduced by the multi-path channel through, which the signal is propagated. The main idea is to append the last part of the OFDM time-domain waveform from the back to the front to create a guard period. The duration of the guard period T_g should be longer than τ_{max} , where τ_{max} designed the Channel Impulse Response (CIR) of the target multi-path environment. The total duration of the OFDM symbol is $T_{tot} = T_s + T_g$.

Furthermore, Multiple-Input Multiple-Output (MIMO) system is an array of N_t transmit antenna and N_r receive antenna. Such systems are used to improve wireless systems capacity, range and reliability. Several applications, based

on MIMO technology, have been proposed in various communication standards as Worldwide Interoperability for Microwave Access (WiMax), evolved High-Speed Packet Access (HSPA+), Wireless Fidelity (WiFi), 3rd and 4th generation of mobile network and Long-Term Evolution (LTE). MIMO system offers a way to increase data throughput and link range without additional bandwidth or increased transmit power. In order to achieve this goal, MIMO system spread the same total transmit power over different transmit antennas to improve the spectral efficiency (Spatial Multiplexing (SM)). On the other hand, MIMO uses Space Time Coding (STC) in order to improve the link reliability.

- 1) Spatial Multiplexing technique (SM): The Spatial multiplexing is a transmission technique in MIMO wireless communication used to transmit independent and separately encoded data streams, from each of the multiple transmit antennas. This technique is used in order to increase the throughput of such wireless communication system. Therefore, the space dimension is reused, or multiplexed, more than one time. If the transmitter is equipped with N_t antennas and the receiver has N_r antennas, Foshini et al. [5] and Telatar [6] have shown that the theoretical capacity of the MIMO channel, with N_t and N_r configuration, grows linearly with $\min(N_t, N_r)$ rather than logarithmically. The channel capacity of a MIMO system is defined by (1) [5] [6]:

$$C = \log_2 \left[\det \left(I_{N_r} + \frac{\rho}{N_t} H H^\dagger \right) \right] \text{bps/Hz.} \quad (1)$$

with

- N_t : Number of transmit antennas.
- N_r : Number of receive antennas.
- I_{N_r} : Identity matrix $N_r \times N_r$.
- $(\cdot)^\dagger$: Conjugate transpose.
- H : MIMO channel matrix $N_t \times N_r$.
- $\rho = \frac{P}{N_o \cdot B}$: Signal to noise ratio (SNR).
- P : Total transmitted power.
- N_0 : Power Spectral Density (PSD).

- 2) Spatial Diversity technique (SD): Spatial diversity technique rely on transmitting simultaneously, redundant copies of data stream on different transmit antennas. The receiver combines the multiple copies of data on each of the received antennas, due to this combination, the error rate of retrieved data will be pretty much less [7]. Space Time Code (STC) is the technique to exploit spatial diversity, which may be split into two main types:

- Space-Time Trellis Codes (STTCs) [8]: This technique is used to distribute a trellis code over multiple transmit antennas and multiple time-slots, furthermore, it provides both coding gain and diversity gain.
- Space-Time Block Codes (STBCs): The STBC is a technique to transmit multiple copies of a data stream across N_t transmit antennas in a MIMO

system. It exploits the spatial diversity and increases the reliability of transmission. This type of code is divided into three main approaches [9]: OSTBC (Orthogonal Space-Time Block Codes), NOSTBC (Non-Orthogonal Space-Time Block Codes) and QSTBC (Quasi-Orthogonal Space-Time Block Codes).

In this paper, we will focus on spatial diversity technique using STBC (Space-Time Block Code) with Alamouti [10] encoder.

The combination of MIMO-OFDM systems are used to reach the higher data rate transmission or improve the spectrum efficiency of wireless link reliability in wireless communication systems. The main challenges of such systems is the synchronization between transmitter and receiver. Two main types of synchronization are necessary, the frequency and the timing synchronization. The frequency synchronization is to correct the phase error caused by the mismatch of the local oscillator (LO) between transmitter and receiver [11] or due to the Doppler effect. On the other hand, Timing synchronization is divided into frame timing synchronization (Coarse timing synchronization) and symbol timing synchronization (Fine timing synchronization). Frame timing synchronization used to detect the arrival of the OFDM frame and symbol timing synchronization is needed in order to detect the beginning of each OFDM symbols on each frame. Here we focus on symbol timing synchronization in MIMO-OFDM systems.

In the literature, several synchronization approaches have been proposed for OFDM and MIMO-OFDM systems [1], [12]–[20]. The main idea is to find a good synchronization preamble, at the transmitter, in order to detect the packet arrival, at the receiver.

In this paper, we propose a robust timing synchronization preamble for MIMO-OFDM systems using orthogonal CAZAC (Constant Amplitude Zero Auto-Correlation) sequences. The CAZAC sequences [21] have constant amplitude and zero autocorrelation for all non-zero shifts. The main characteristics of CAZAC sequences are their correlation functions. They have a good autocorrelation function and their crosscorrelation function is near zero. Due to their orthogonality, CAZAC sequences reduce inter-code interference between multiple antennas and have a lower PAPR. As a result, CAZAC sequences are regarded as optimum preamble for timing synchronization in MIMO-OFDM systems.

This paper is organized as follows. Section II describes the MIMO-OFDM system based on STBC code. Existing approaches and related work are presented in Section III. Section IV presents the criteria for selecting a good synchronization sequences. The working principle of the proposed method and the different preamble structure is presented in Section V. Simulation results and conclusion are discussed in

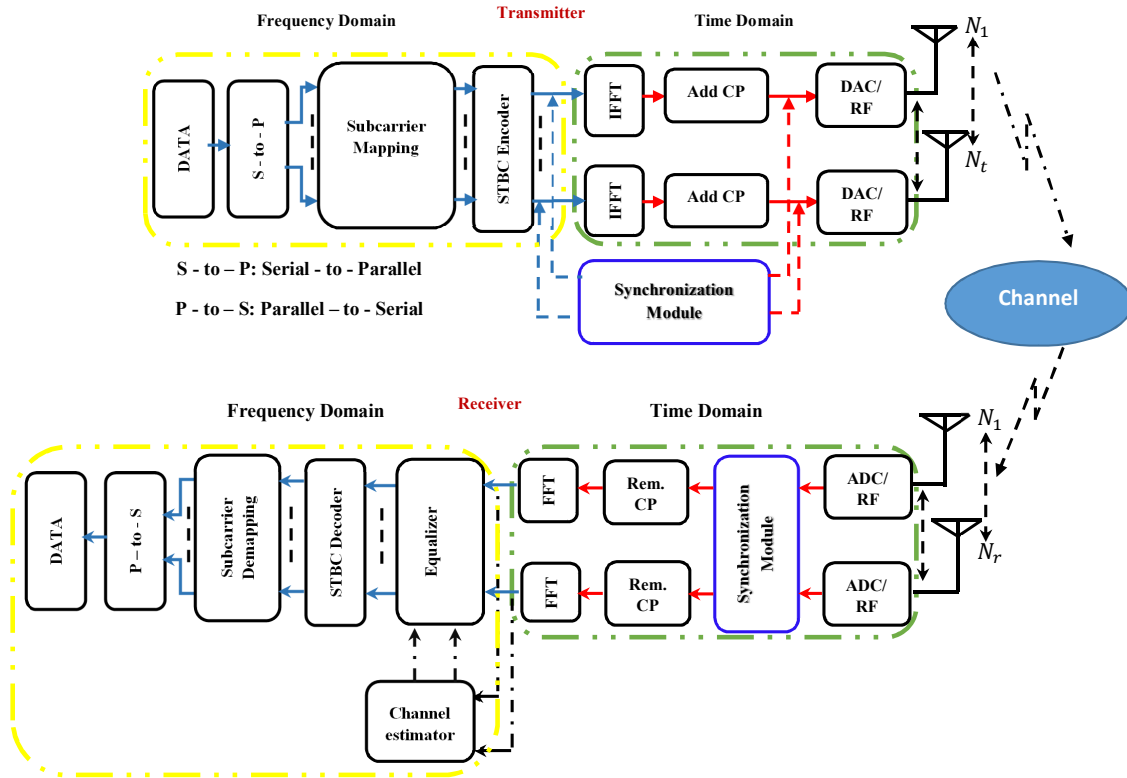


Fig. 1: Block diagram of MIMO-OFDM-STBC transmitter and receiver

Sections VI and VII, respectively.

II. MIMO-OFDM SYSTEM ARCHITECTURE

Basically, MIMO-OFDM radio communication system consists of a transmitter, a channel, and a receiver. In this section, we present the different parts of MIMO-OFDM communications system. The transmitter generates OFDM symbols, which are modulated using M-air modulation, then, they are transmitted over multiple transmit antennas using STBC block [9] [10]. Figure 1 presents a general MIMO-OFDM system model with N_t transmit antennas, N_r receive antennas and N_{sc} subcarriers per transmit antenna.

A. MIMO-OFDM transmitter

The first part of MIMO-OFDM system is the transmitter. In a OFDM transmitter, information data are transmitted blockwise. The first block is a data block where several serial stream of data are generated. Then, a serial to parallel block (S-to-P) converts the serial data stream to parallel data stream. Subcarrier Mapping block is used in order to map parallel data stream to complex symbols. This block uses different constellation mapping either Phase Shift Keying (PSK) or Quadrature Amplitude Modulation (QAM). After mapping, complex symbols are then introduced into a STBC encoder (in this approach we use Alamouti Encoder). Then, we use IFFT to modulate the parallel data stream in order to generate the OFDM symbols over different transmit antennas.

After performing IFFT, the data is again converted into serial stream. A cyclic prefix block named Add CP consists to insert a Cyclic Prefix (CP) or Guard Interval (GI), which is appended at the start of the serial stream. The cyclic Prefix is actually an exact copy of the last part or T_G samples of the data. The purpose of CP is to remove the ISI and channel effects. The synchronization block is used in order to insert the synchronization preamble at the beginning of each OFDM frame. Two different approaches are presented, the synchronization preamble is appended in frequency domain [16] [20] or in time domain [19]. In this paper, we focus on the first approach.

The transmitted OFDM signal s_i on each transmit antenna T_i is given by:

$$s_i(t) = \frac{1}{\sqrt{N_{sc}}} \sum_{k=0}^{N_{sc}-1} \Re \{ x_k e^{j \cdot 2\pi \cdot f_k \cdot t} \} \quad (2)$$

where x_k is the symbol on the frequency f_k .

B. MIMO channel Model

The modelling of a practical MIMO channel includes the transmit vector, receive vector, multi-path channel matrix and Noise. The MIMO channel model between the transmit antenna T_i and receive antenna R_j , where $i \in \{1, N_t\}$ and $j \in \{1, N_r\}$, is given by:

$$H(t) = \sum_{l=1}^L H_l \delta(t - \tau_l) \quad (3)$$

where H_l are the matrix coefficients of the l^{th} path. This matrix is $N_t \times N_r$. δ represents the pulse function and L is the maximum number of multi-paths. H_l is given by:

$$H_l = \begin{bmatrix} h_{1,1}^l & h_{1,2}^l & \dots & h_{1,N_r}^l \\ h_{2,1}^l & h_{2,2}^l & \dots & h_{2,N_r}^l \\ \vdots & \vdots & \ddots & \vdots \\ h_{N_t,1}^l & h_{N_t,2}^l & \dots & h_{N_t,N_r}^l \end{bmatrix} \quad (4)$$

C. MIMO-OFDM Receiver

The second part of MIMO-OFDM system is the receiver. The receiver is exactly the reverse of transmitter. The first block after the analog to digital converter (ADC) is the timing synchronization block. After a good timing synchronization, the cyclic prefix of each OFDM symbol is removed. After removing CP, we perform Fast Fourier Transform (FFT) to return the data back into frequency domain. The data is then fed into the equalizer and channel estimator. After equalization, the data are decoded by STBC decoder. Then, a Subcarrier De-mapping block is presented in order to demodulate and recover the binary information. The parallel to serial (P-to-S) converter allows to reformatting the binary bit stream.

The received signal r_j on each receive antenna R_j is given by:

$$\begin{aligned} r_j(t) &= \sum_{i=1}^{N_t} [h^{i,j}(\tau, t) \star x_i(t)] + n_{ij}(t) \\ &= \frac{1}{\sqrt{N_{sc}}} \sum_{i=1}^{N_t} \sum_{p=1}^{P_{ij}} \left[\alpha_p(t) e^{-j2\pi f_k \tau_p(t)} \star \right. \\ &\quad \left. s_i[\tau - \tau_p(t)] \right] e^{j2\pi f_k t} \\ &\quad + n_{ij}(t) \end{aligned}$$

where h_{ij} is the channel between the transmit antenna T_i and the receive antenna R_j , τ is the propagation delay for the different channels paths, α_p is the attenuation for the p^{th} path, $s_i(t)$ is the OFDM transmitted signal, P_{ij} is the number of path between T_i and R_j and n_{ij} is the Additive white Gaussian noise (AWGN) noise between T_i and R_j .

III. RELATED WORK

In the literature, several synchronization approaches have been proposed for MIMO-OFDM, as shown in Section I. The most of the synchronization methods are preamble based, that means, the header of each OFDM frame contains a known preamble structure. As in [22], authors provide a preamble structure based on Loosely Synchronous (LS) codes for timing and frequency synchronization for a MIMO-OFDM

system. This preamble is used in order to detect the beginning of each received frame. The main characteristics of LS codes is to have a good autocorrelation and cross-correlation functions within certain vicinity of the zero shifts. In this method, the synchronization process is divided into four stages. The first and the second stage are used in order to estimate the coarse timing synchronization and the coarse frequency synchronization, respectively. The third stage is to detect the beginning of each OFDM symbols in each frame and estimate the channel parameters. the fourth step is used for the fine frequency estimation. The main drawback of this method is the structure of preambles, where it is relatively complex. Another disadvantage of this method is the different stage used in order to detect the beginning of frame.

Another approach proposed in [23] based on Orthogonal Variable Spreading Factor (OVSF) for timing synchronization. In this approach, a Multiple Input-Single Output (MISO) systems 2×1 is considered. The length of each OFDM symbol and their CP is 256 and 32, respectively. The synchronization preamble has the same length as the CP is appended at the beginning of each OFDM frame. As result, this approach shows that for MISO-OFDM systems 2×1 , the timing acquisition probability is 1 for an $SNR \geq -5 dB$. Here, timing acquisition probability describes the probability to detect the timing synchronization point. The main drawback of this approach is that the synchronization preamble is appended in the time domain. With such hardware implementation, authors need an extra block to insert the preamble in time domain, while, in frequency domain their is no need to this block due to the IFFT.

Based on Schmidl and Cox's approach [12], Farhan proposed in [24] a modified approach that is not using the training sequence and making cyclic prefix (CP) as the reference in order to obtain efficiency in transmitting power. This approach uses the sliding window technique to compute the correlation of the received signal with the cyclic prefix. The main drawback of this method is the correlation with the CP in multipath fading channel. In such channel, when the receiver receives several delayed path with CP, the timing metric obtained by the correlation shows more correlation peak, then the receiver would not able to detect the start of OFDM frame.

A compact preamble design for synchronization in distributed MIMO-OFDM systems has been proposed in [25]. In this approach, a preamble structure based on exclusive sub-band has been proposed. Adjacent sub-bands are spaced by a guard bands to reduce the interference between sub-bands. The total length of the proposed preamble based on CAZAC sequences has the same length as an OFDM symbol. The simulation results shown that for a MISO-OFDM (3×1), the acquisition probability for timing synchronization is 70% for an $SNR = 5 dB$. In this work, we compare the simulation results of our proposed approach with those of the method

proposed by Chin-Liang et al. [25].

The proposed method in [25] suffers from several disadvantages, mainly the complexity to generate the preamble structure for a large number of transmit antennas. In [25], when the number of transmit antennas increases, the size of sub-bands should be reduced to take into account all transmit antennas. Therefore, at the receiver, the acquisition probability for timing synchronization decreases due to the length of synchronization sequence.

IV. OPTIMAL TRAINING SEQUENCES FOR TIMING SYNCHRONIZATION

Timing synchronization methods are performed using training sequences at the beginning of each OFDM frame in MIMO-OFDM systems. The main characteristic of training sequences is to have good autocorrelation and cross-correlation properties. At receiver, this characteristic provides a good detection of a correlation peak as closed as possible to a Dirac pulse. The main training sequences used in the state of art are listed below.

A. Gold sequences

Gold sequences [26] of length N are constructed using a preferred pair of Pseudorandom Noise (PN) sequences. Let a and b are two preferred pair of m -sequences, those sequences have a three valued correlation function:

$$\theta_{(a,b)} = -1, -t(m) \text{ or } t(m) - 2 \quad (5)$$

where

$$t(m) = \begin{cases} 1 + 2^{(m+2)/2} & \text{if } m \text{ is even} \\ 1 + 2^{(m+1)/2} & \text{if } m \text{ is odd} \end{cases} \quad (6)$$

The set of Gold sequences includes the preferred pair of m -sequences a and b , and the mod 2 sums of a and cyclic shifts of b represented by the operator T^{-p} . The set S_{gold} of Gold sequences is given by:

$$S_{gold} = \{a, b, a \oplus b, a \oplus T^{-1}b, \dots, a \oplus T^{-(N-1)}b\} \quad (7)$$

The maximum correlation value for any two Gold sequences in the same set is equal to the constant $t(m)$.

The main advantage of Gold sequence lies in sending such sequences in periodic way to retain the good correlation properties. In synchronization, such sequences are used aperiodically, on the other hand, Gold sequences loses their good correlation properties. The autocorrelation and cross-correlation functions of aperiodic Gold sequences are shown in Figure 2, where index represents indices at which the correlation was estimated.

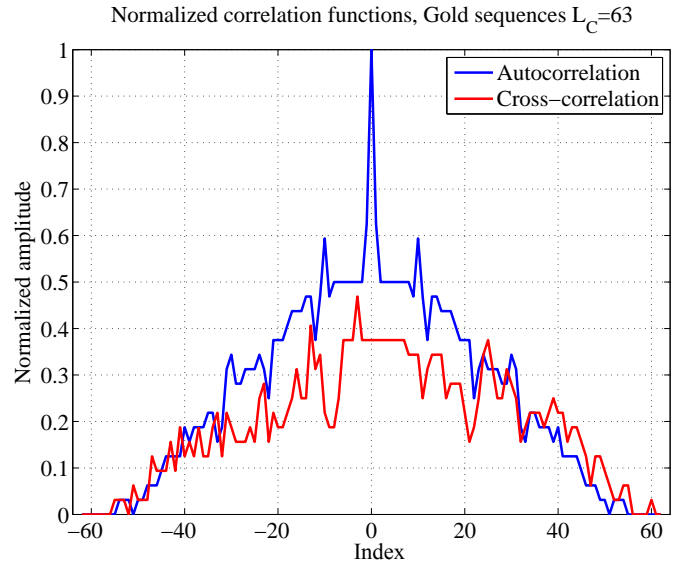


Fig. 2: Autocorrelation and cross-correlation of Gold sequence, $N = 63$

B. Walsh-Hadamard code

Another generation of code called Walsh-Hadamard code. Such codes are orthogonal and built from an initial Hadamard's matrix [27]. Hadamard's matrices are given by:

$$H_1 = [1], H_2 = \begin{bmatrix} 1 & 1 \\ 1 & -1 \end{bmatrix}, \dots, H_{2^k} = \begin{bmatrix} H_{2^{k-1}} & H_{2^{k-1}} \\ H_{2^{k-1}} & -H_{2^{k-1}} \end{bmatrix} \\ = H_2 \otimes H_{2^{k-1}} \text{ for } 2 \leq k \in \mathbb{N} \quad (8)$$

where \otimes denotes the Kronecker product. An Hadamard matrix H_n satisfies the following property:

$$H_n \cdot H_n^T = nI_n$$

where H_n^T is the conjugate transpose of H_n and I_n is a $n \times n$ identity matrix.

The main advantage of Hadamard code is the orthogonality between the different code. On the other hand, the autocorrelation function for some code has secondary peak as shown in Figure 3.

C. CAZAC sequences

A Constant Amplitude Zero Auto-Correlation (CAZAC) sequence [28] $c(m)$ is a complex sequence and has constant magnitude, $|c(m)| = 1$ for $m \in [0, L_C - 1]$ where $L_C = 2^n$ is the finite length of $c(m)$, $n \in \mathbb{N}$, and has zero-autocorrelation function with shifted version of the same sequence. The cross-correlation function of CAZAC sequences has a value near to zero.

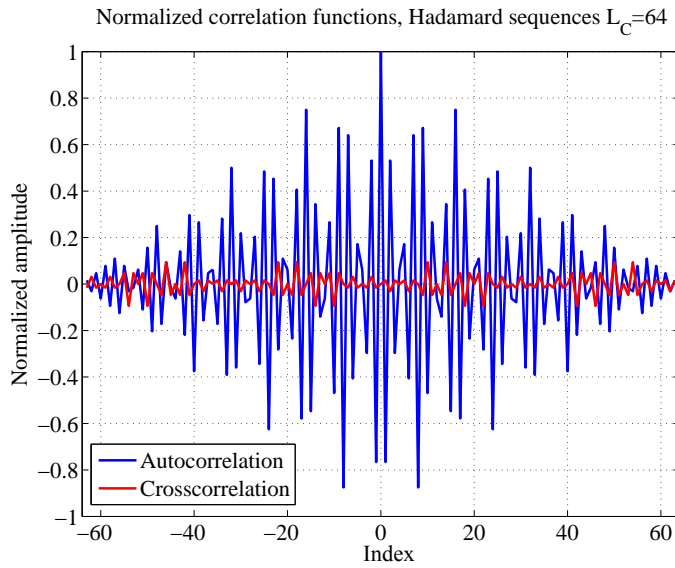


Fig. 3: Autocorrelation and cross-correlation of Hadamard sequence, $L_C = 64$

Let $C(k)$, in frequency domain, be a CAZAC sequence of length L_C , $C(k)$ is given by:

$$C(k) = \begin{cases} e^{j\left(\frac{\pi P k(k+1)}{L_C}\right)} & \text{if } k \text{ is odd} \\ e^{j\left(\frac{\pi P k^2}{L_C}\right)} & \text{if } k \text{ is even} \end{cases} \quad (9)$$

where $P \in \mathbb{N}$ is a prime number with L_C and $k \in \{0, L_C - 1\}$ is the index of the sample.

After IFFT algorithm, the corresponding sequence of $C(k)$ in the time domain ($c(m)$), is given by:

$$c(m) = \frac{1}{L_C} \sum_{k=0}^{L_C-1} C(k) \cdot e^{j\left(\frac{2\pi}{L_C}\right)mk}, m \in [0, L_C - 1] \quad (10)$$

The normalized autocorrelation and cross-correlation functions of CAZAC sequences of length $L_C = 64$ are shown in Figure 4.

D. Optimal sequence selection

In MIMO system, unlike Single Input Single Output (SISO) system, we need to send several data at one time according the number of transmit antennas. In this context, the optimal training sequences should have a good autocorrelation and crosscorrelation functions in order to distinguish the different received signal at the receiver. Gold sequences have a good autocorrelation function, on the other hand, they have a high value for their cross-correlation function. Hadamard sequences have a good autocorrelation and crosscorrelation functions

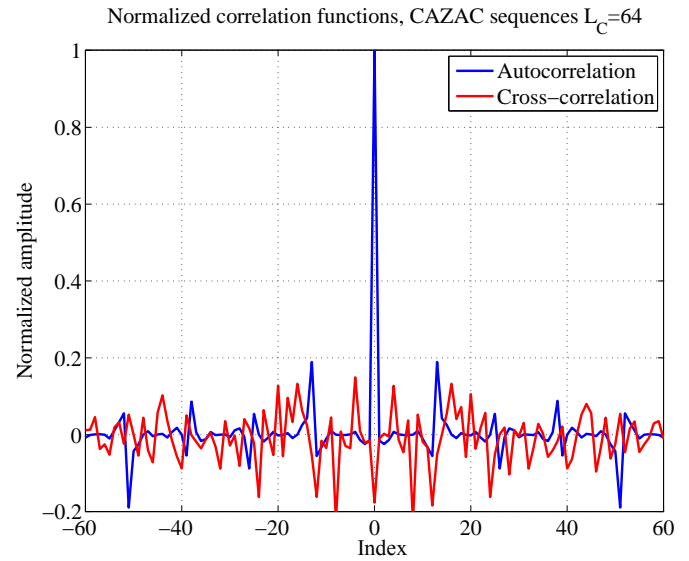


Fig. 4: Autocorrelation and cross-correlation of CAZAC sequence, $L_C = 64$

due to their orthogonality, while, for some sequences, the autocorrelation has secondary correlation peaks. On the other hand, CAZAC sequences show a good autocorrelation and crosscorrelation functions due to their orthogonality and complex value. After a comparison between the characteristics of different sequences, our work was focused on the use of CAZAC sequence as training sequences for timing synchronization in MIMO-OFDM systems.

V. PROPOSED TIMING SYNCHRONIZATION PREAMBLE

In this section, based on [1], we propose our robust timing synchronization preamble in MIMO-OFDM systems based on CAZAC sequence. Let C be a CAZAC sequence of length L_C , where L_C represents the size of synchronization preamble divided by 2, in other term $L_C = L_{FFT}/2$ where L_{FFT} is the size of the FFT, and C^* denotes the conjugate of C . We propose in this section two different structures, as follows.

A. First preamble structure

The timing synchronization preamble is generated in frequency domain, then it is added at the beginning of each OFDM frame according to transmit antenna. Figure 5 shows the structure of the first proposed preamble in frequency domain over different transmit antennas.

The preamble structure in Figure 5 relies in sending a CAZAC sequence (C) over the odd subcarrier, in frequency domain, and C^* on the even subcarrier. The preamble ϕ^i that transmitted on the i^{th} transmit antenna is given by the following equation:

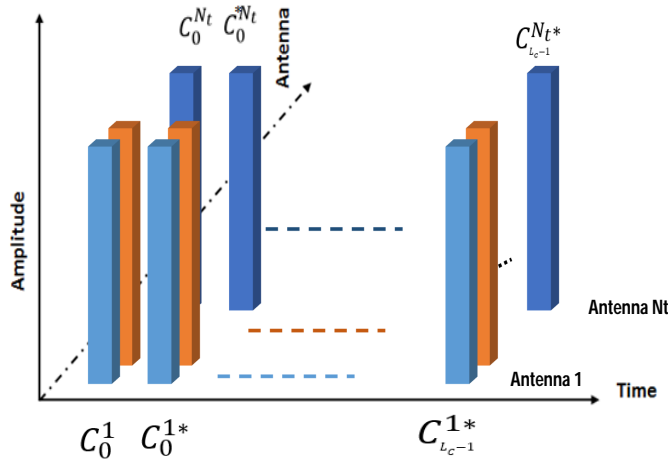


Fig. 5: First preamble structure in frequency domain over different transmit antennas

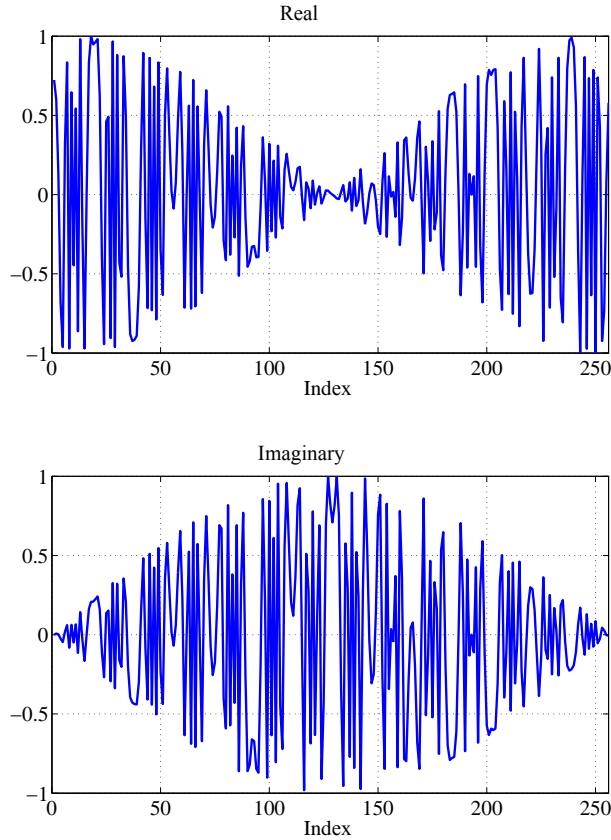


Fig. 6: Real and imaginary parts of the first preamble structure in time domain

$$\varphi^i(k) = \begin{cases} C^i\left(\frac{k}{2}\right) & \text{if } k \bmod 2 = 0 \\ C^{i*}\left(\frac{k-1}{2}\right) & \text{if } k \bmod 2 \neq 0 \end{cases} \quad (11)$$

where $k \in \{0, L_{FFT} - 1\}$ and $L_{FFT} = 2 \cdot L_C$.

The term C_k^i is the sample of the CAZAC sequence carried by the k^{th} subcarrier and transmitted by the transmitting antenna T_i . The proposed method can be applied regardless of the number of transmit or receive antennas.

Figure 6 shows the real and imaginary parts of timing synchronization preamble in time domain.

The combination of a CAZAC sequence C with its conjugate C^* gives a time-domain complex envelope form that have a good autocorrelation and cross-correlation functions. This combination does not destroy the orthogonality between subcarriers, and it retains the orthogonality between different preambles over different transmit antennas.

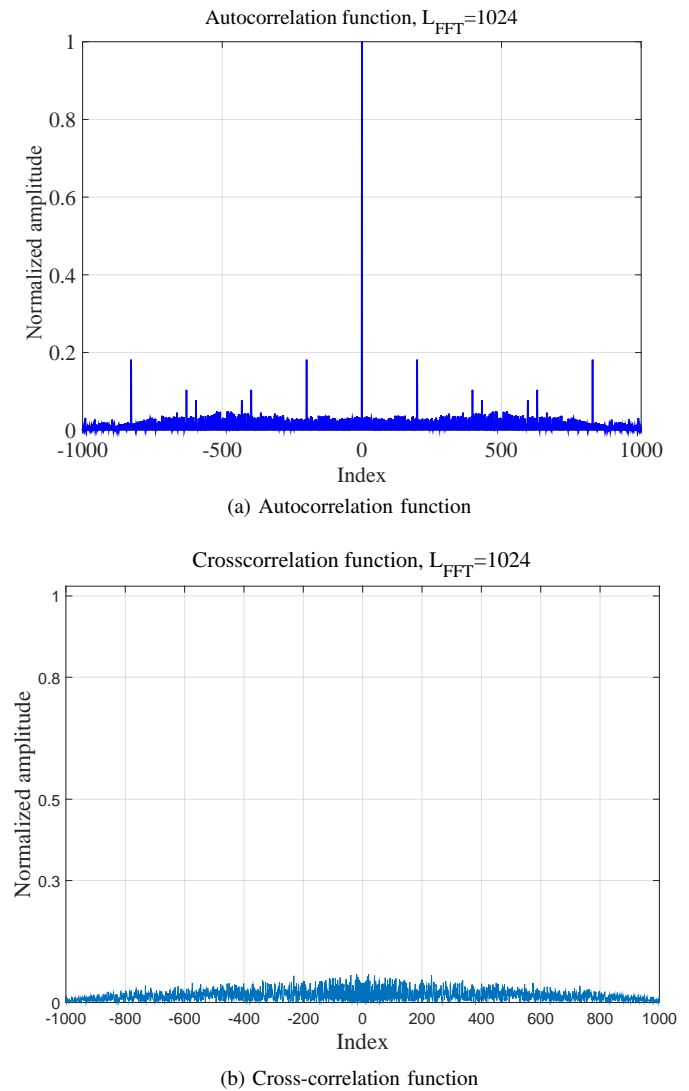


Fig. 7: Autocorrelation and cross-correlation functions of the first preamble structure ($L_{FFT} = 1024$)

Figure 7 presents the autocorrelation (Figure 7a) and the

cross-correlation (Figure 7b) functions of the first preamble structure. This preamble shows a good correlation functions in order to detect the timing synchronization peak.

B. Second preamble structure

The second preamble structure consists of dividing the preamble into two parts of length $L_C = L_{FFT}/2$ each one. The first part contains an entire CAZAC sequence C of length L_C , while, the second part contains the conjugate of C denoted C^* . Figure 8 presents the preamble structure over different transmit antennas in frequency domain.

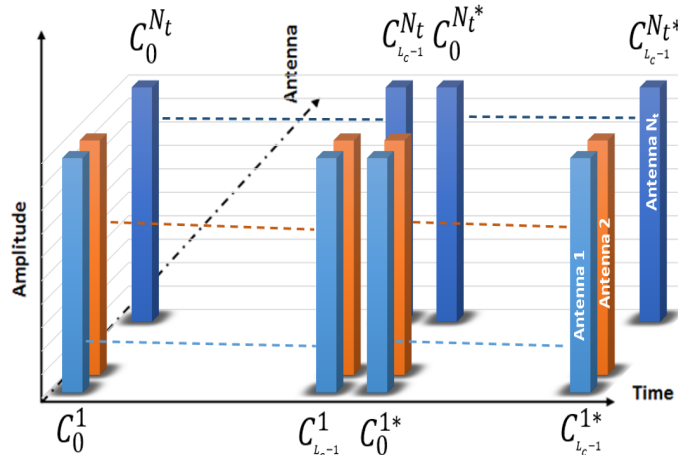


Fig. 8: Second preamble structure in frequency domain over different transmit antennas

Figure 9 presents the autocorrelation and cross-correlation functions of the second preamble structure in time domain.

Let φ^i be the preamble sent on the i^{th} transmit antenna, the equation of this preamble in frequency domain is given by:

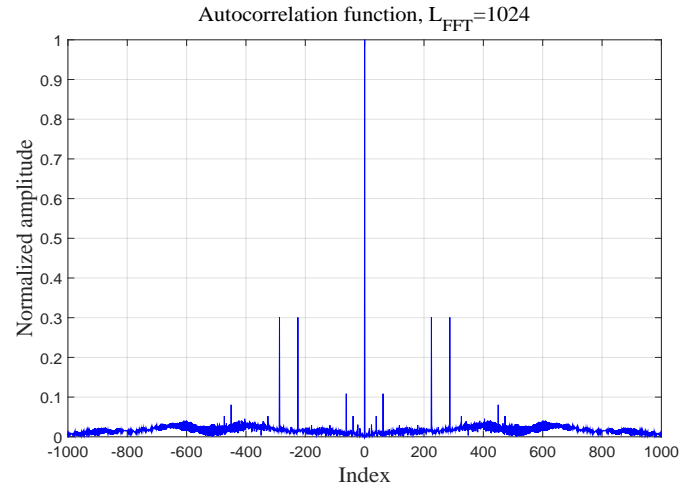
$$\varphi^i(k) = \begin{cases} C^i(k) & \text{if } 0 \leq k < L_C \\ C^{i*}(k - L_C) & \text{if } L_C \leq k < L_{FFT} \end{cases} \quad (12)$$

VI. SIMULATIONS RESULTS

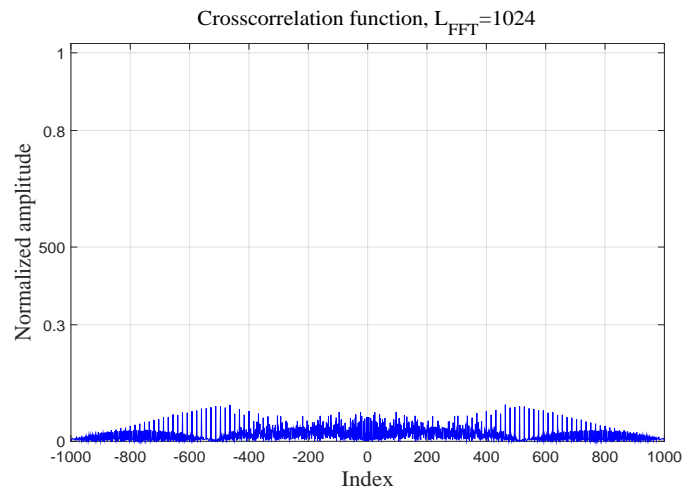
In this section, we present the simulation parameters and simulation results for different preamble's structure in AWGN channel and multipaths fading channel, in order to evaluate the performance of our proposed preambles against [25].

A. System specifications & simulation parameters

In order to improve the simulation results, we simulate our preamble structures with different system specification and simulation parameters. Simulations results are done with SISO-OFDM and MIMO-OFDM systems up to 8×8 . On the other hand, the OFDM system consists of 512 and 1024 subcarriers, where $L_{FFT} = \{512, 1024\}$, respectively. The channel model was considered as Rayleigh multipath



(a) Autocorrelation function



(b) Cross-correlation function

Fig. 9: Autocorrelation and cross-correlation functions of the second preamble structure ($L_{FFT} = 1024$)

fading channel with 6 paths sample-spaced with T_s , where T_s describes the sampling time; this channel is suggested by the IEEE 802.11 Working Group [29]. Other simulation parameters are summarized in Tables I and II.

TABLE I: System Specifications and Requirements

| Parameters | Justification | |
|------------|---------------|--|
| | Value | Description |
| System | 8×8 | SISO and MIMO-OFDM system up to 8×8 |
| L_{FFT} | 1024 & 512 | Length of IFFT/IFFT |
| L_{CP} | $L_{FFT}/4$ | Length of Cyclic Prefix |
| Sequences | CAZAC | Type of synchronization sequences |
| L_C | $L_{FFT}/2$ | Length of synchronization sequences |
| SNR in dB | 0 to 25 | SNR over all the OFDM Frame |

B. Timing synchronization algorithm

The main drawback of the most of timing synchronization algorithm is the complexity of frames and symbols detection.

TABLE II: Power profile and channel model

| Simulation Parameters | Value |
|---|--|
| Channel Type | Multi-path Rayleigh and AWGN channel |
| Number of channel taps between different antennas | 6 |
| Propagation delay between different multipath | $[0.T_s, 1.T_s, 2.T_s, 3.T_s, 4.T_s, 5.T_s]$ |
| The power of each multipath | $[0.8111, 0.1532, 0.0289, 0.0055, 0.0010, 0.0002]$ |

Our proposed method consists of detecting coarse and fine timing synchronization in one operation, this is the main advantage of our proposed method. We implement at each receiver a correlation function \mathcal{R}_{r_j, seq_j} in order to detect the timing synchronization peak between the received signal r_j and the local sequence seq_j generated by the receive antenna R_j . This correlation is done in time domain. Due to the mapped CAZAC sequence (C and C^*) in each preamble, the correlation between received signal and local sequence may give a high peak's value, this function is calculated as following:

$$\mathcal{R}_{r_j, seq_j}(n) = \sum_{n=0}^{L_{FFT}-1} [r_j(n) * seq_j(n - \tau)] \quad (13)$$

where n is the index of the sample. The correlation function \mathcal{R}_{r_j, seq_j} feed into an estimator in order to detect the coarse timing synchronisation. The timing synchronization estimate is given by:

$$\hat{ind}_n = \underset{n}{\operatorname{argmax}} \{ \|\mathcal{R}_{r_j, seq_j}(n)\| \} \quad (14)$$

where n is considered as the coarse timing synchronization point. At the same time, and, by shifting the FFT window, we can find the fine timing synchronization or the beginning of each OFDM symbol on each frame. Let P_{SYNC} describes the timing synchronization acquisition probability. P_{SYNC} presents the probability of successful timing synchronization at receiver.

C. Simulation results for the first preamble structure

Simulation results for all preamble structures, are done using simulation parameters in Tables I and II. Figures 10 and 11 show the acquisition probability for different SISO and MIMO-OFDM systems, where the length of preamble are $L_{FFT} = 1024$ and $L_{FFT} = 512$.

Figure 10 presents a good timing synchronization for a low SNR. For an $SNR = -5dB$, the $P_{SYNC} \geq 90\%$ for all MIMO-OFDM system up to 8×8 . Therefore, for an $SNR = 0dB$, the proposed timing synchronization preamble shows a perfect timing synchronization for SISO-OFDM system. The $P_{SYNC} \geq 97\%$ for MIMO-OFDM system 2×2 for the same SNR. For a MIMO-OFDM system 4×4 the $P_{SYNC} \geq 96\%$ at an $SNR = 5dB$. On the other hand, for MIMO-OFDM system 8×8 , the acquisition probability

P_{SYNC} reaches 98% at an $SNR = 10dB$.

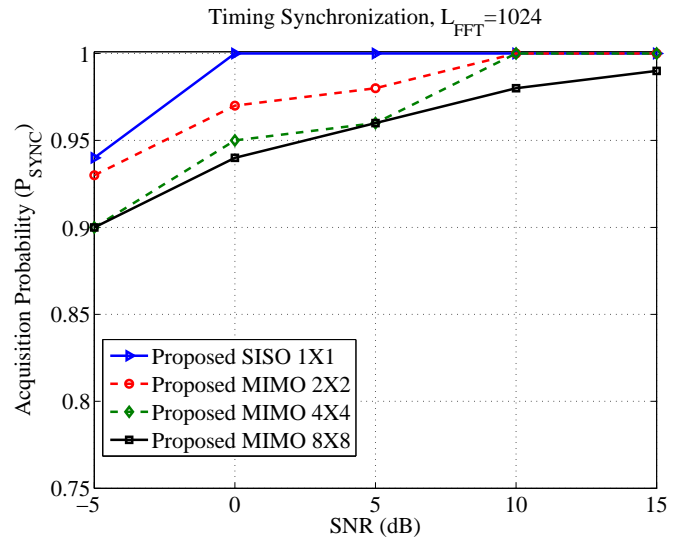


Fig. 10: Timing synchronization performance of the first proposed preamble with $L_{FFT} = 1024$

Figure 11 presents the performance of our synchronization preamble of length $L_{FFT} = 512$. In this figure, the acquisition probability P_{SYNC} is greater than 97% for both SISO-OFDM and MIMO-OFDM 2×2 systems at an $SNR = 0dB$. Therefore, $P_{SYNC} \geq 90\%$ for MIMO-OFDM 4×4 system at an $SNR = 0dB$. On the other hand, the P_{SYNC} reaches 80% at an $SNR = 5dB$ for MIMO-OFDM system 8×8 .

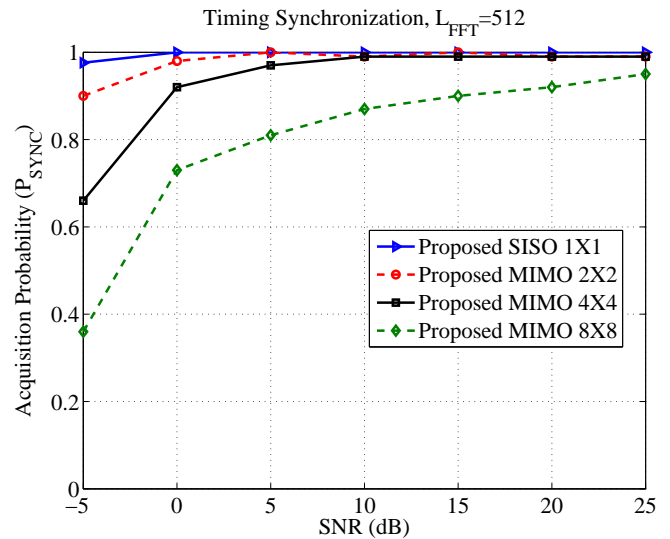


Fig. 11: Timing synchronization performance of the first proposed preamble with $L_{FFT} = 512$

Table III summarizes the simulation results of Figures 10 and 11. It can be shown that the performance of our timing synchronization method increases with the length of L_{FFT} .

TABLE III: Comparison between the acquisition probability of different MIMO-OFDM systems, in term of SNR and length of FFT

| MIMO-OFDM system | Acquisition probability | | |
|------------------|-------------------------|----------|-----------|
| | P_{SYNC} | SNR (dB) | L_{FFT} |
| MIMO-OFDM 2x2 | $\geq 97\%$ | > 0 dB | 1024 |
| | $\geq 96\%$ | > 0 dB | 512 |
| MIMO-OFDM 4x4 | $\geq 95\%$ | > 0 dB | 1024 |
| | $\geq 93\%$ | > 0 dB | 512 |
| MIMO-OFDM 8x8 | $\geq 94\%$ | > 0 dB | 1024 |
| | $\geq 78\%$ | > 0 dB | 512 |

Moreover, the results of Figure 10 ($L_{FFT} = 1024$) show a good performance against those presented in Figure 11 ($L_{FFT} = 512$).

In order to evaluate the performance of our proposed method, we conducted an extensive comparison of our approach with the synchronization scheme of [25]. Hung and Chin Wang [25] used a subband-based preamble based on CAZAC sequences. The main drawback of this method is the number of transmit antennas. As the number of transmit antennas increases, the length of synchronization sequence, on each transmit antenna, decreases. Therefore, the value of the synchronization peak at the receiver decreases.

Figure 12 presents the performance between our proposed approach and the synchronization scheme of [25]. Simulation results in Figure 12 are done with the simulation parameters of Tables I and II with a synchronization preamble of length $L_{FFT} = 256$, and MIMO-OFDM system 2×2 and 3×3 .

Simulation results of our proposed approach have a good performance against [25] at a low SNR. The acquisition probability P_{SYNC} for our method is greater than 90% at an $SNR \geq 5$ dB for both MIMO-OFDM 2×2 and 3×3 system. Therefore, the proposed method in [25] shows that the acquisition probability is between 0.5 and 0.75 at the same value of SNR.

D. Simulation results for the second preamble structure

This section presents the simulation results for the second preamble structure. Simulation results are done performed using the simulation parameters in Tables I and II. The acquisition probabilities (P_{SYNC}) for different length of synchronization preamble ($L_{FFT} = 1024$ and $L_{FFT} = 512$) are shown in Figures 13 and 14, respectively.

Figure 13 shows that for a $L_{FFT} = 1024$ and a $SNR \geq -5$ dB, the acquisition probability P_{SYNC} is greater than 95% for both SISO-OFDM and MIMO-OFDM 2×2 systems. Otherwise, both systems have a perfect P_{SYNC} for

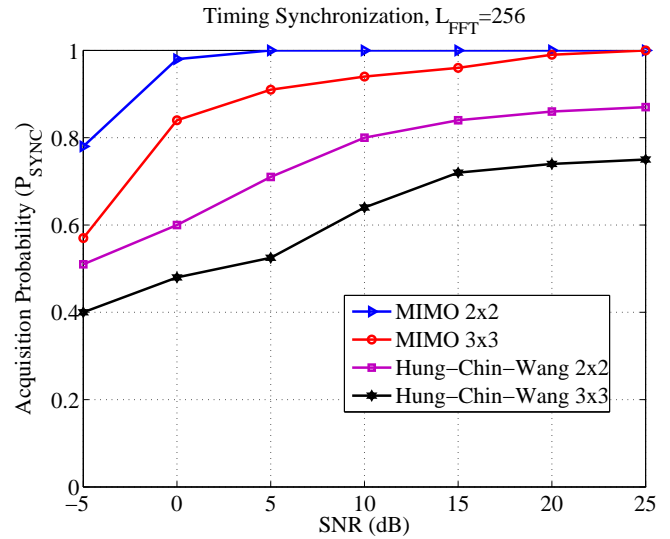


Fig. 12: Comparisons between the proposed approach and subband-based preamble [25]

an $SNR \geq 5$ dB. On the other hand, MIMO-OFDM 4×4 system has a P_{SYNC} greater than 94% for a $SNR \geq 0$ dB, this system has a perfect P_{SYNC} for a $SNR \geq 15$ dB. Therefore, the acquisition probability for MIMO-OFDM 8×8 system, reaches 90% for an $SNR > 2$ dB.

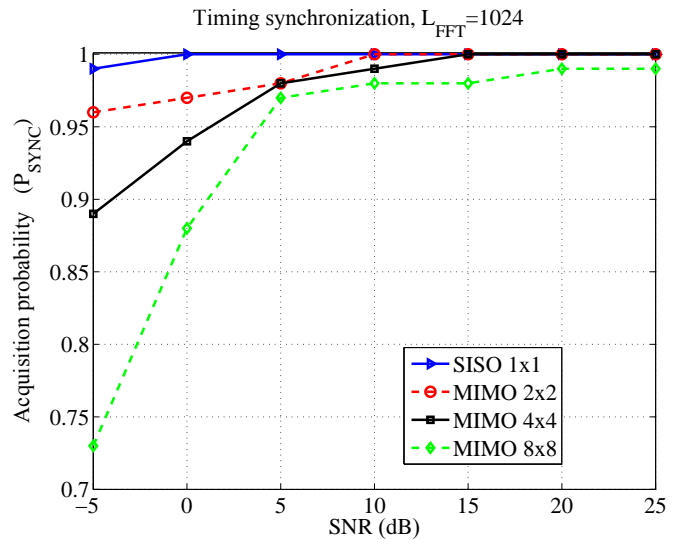


Fig. 13: Timing synchronization performance of the second proposed approach ($L_{FFT} = 1024$)

Figure 14 presents the performance of timing synchronization method for a $L_{FFT} = 512$. As shown in this figure, at an $SNR = 0$ dB, both SISO-OFDM and MIMO-OFDM 2×2 systems have the acquisition probability $P_{SYNC} > 95\%$, and $P_{SYNC} > 90\%$ for MIMO-OFDM 4×4 system. Furthermore, for MIMO-OFDM 8×8 system the P_{SYNC} reaches 70% for

the same SNR .

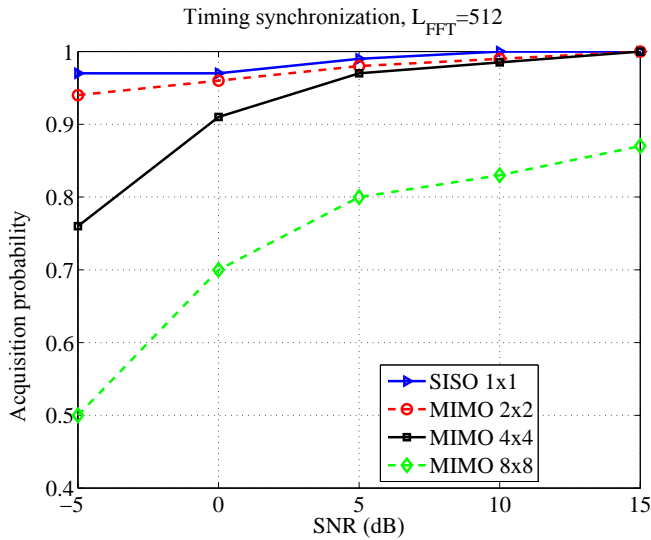


Fig. 14: Timing synchronization performance of the second proposed approach ($L_{FFT} = 512$)

In order to show the performance of our approach clearly, simulation results of our approach are compared with the method proposed in [25], using the same simulation parameters of Tables I and II. The comparison results are shown in Figure 15, where the preamble size is $L_{FFT} = 256$. As shown in this figure, the timing synchronization acquisition probability for our proposed approach is better than the proposed method in [25] even for a low SNR .

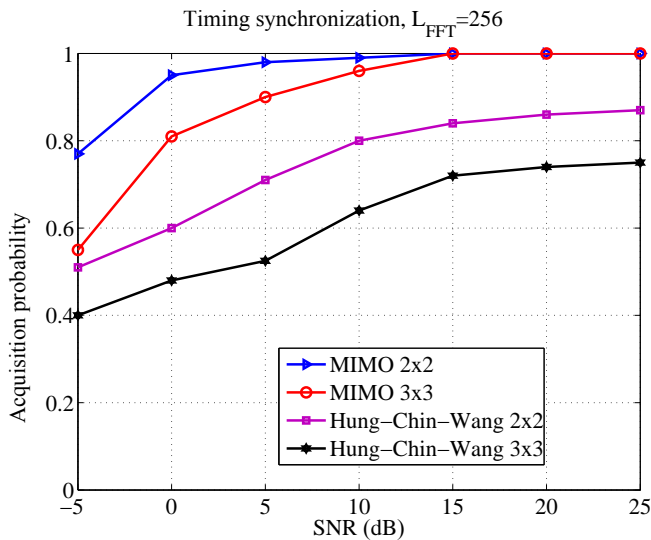


Fig. 15: Comparisons between the second proposed approach and subband-based preamble proposed in [25]

For an $SNR = 0$ dB, for both MIMO-OFDM systems 2×2 and 3×3 , our proposed approach has a $P_{SYNC} > 0.8$, while for Hung-Chin's method the P_{SYNC} not exceed 0.6 for both systems.

VII. CONCLUSION

In the last year, the telecommunications have been growing in order to present a good quality of services (QoS) and large bandwidth. Furthermore, in order to increase the capacity of channel, or to improve the quality of the link, MIMO-OFDM system was presented. On the other hand, such system has a big challenge, which is the timing synchronization. Timing synchronization means how to detect the beginning of each received frames and each symbols in the frame. In order to detect the timing frame synchronization, we proposed two robust timing synchronization preamble. At the transmitter, a synchronization preamble is appended at the beginning of each OFDM frame. This preamble is based on CAZAC sequences, where those sequences have a good autocorrelation and cross-correlation functions.

At each receiver, the received signal correlated with a local sequence generated by the receiver. Due to the mapped of the orthogonal CAZAC sequences over different subcarriers, a correlation peak will appear in order to detect the beginning of frame. In comparison to the subband preamble based proposed by [25], our timing synchronization approaches present a better timing frame synchronization at a low SNR . Finally, we can perform coarse and fine timing synchronization using the same correlation peak.

In this paper, we can find also a few degradation of performance between our two approach. This degradation is due to the mapped CAZAC sequence on each preamble structure. Hence, as future work, it will be interesting to see the performance of our approach for frequency synchronization.

ACKNOWLEDGMENT

This work was supported by the GET of Lebanese University and IETR of Rennes-France.

REFERENCES

- [1] A. Rachini, A. Beydoun, F. Nouvel, and B. Beydoun, "Timing synchronization method for mimo-ofdm systems with cazac sequences," in INNOV 2014, The Third International Conference on Communications, Computation, Networks and Technologies, 2014, pp. 30–35.
- [2] IEEE Standard 802.11n: Wireless LAN Medium Access Control (MAC) and Physical Layer (PHY) Specifications Amendment 5: Enhancements for Higher Throughput, Institute of Electrical and Electronics Engineers, Oct. 2009.
- [3] L. Cimini, "Analysis and simulation of a digital mobile channel using orthogonal frequency division multiplexing," Communications, IEEE Transactions on, vol. 33, no. 7, July 1985, pp. 665–675.
- [4] S. G. Johnson and M. Frigo, "Implementing ffts in practice," 2009.
- [5] G. J. Foschini and M. J. Gans, "On limits of wireless communications in a fading environment when using multiple antennas," Wireless Personal Communications, vol. 6, 1998, pp. 311–335.
- [6] I. E. Telatar, "Capacity of multi-antenna gaussian channels," European Transactions On Telecommunications, vol. 10, no. 6, Dec. 1999, pp. 585–595.
- [7] I. Khan, S. A. K. Tanoli, and N. Rajatheva, "Capacity and performance analysis of space-time block coded mimo-ofdm systems over rician fading channel," International Journal of Electrical and Computer Engineering, 2009.

- [8] V. Tarokh, N. Seshadri, and A. Calderbank, "Space-time codes for high data rate wireless communication: performance criterion and code construction," *Information Theory, IEEE Transactions on*, vol. 44, no. 2, 1998, pp. 744–765.
- [9] V. Tarokh, H. Jafarkhani, and A. Calderbank, "Space-time block codes from orthogonal designs," *Information Theory, IEEE Transactions on*, vol. 45, no. 5, 1999, pp. 1456–1467.
- [10] S. Alamouti, "A simple transmit diversity technique for wireless communications," vol. 16, no. 8, Oct. 1998, pp. 1451–1458.
- [11] V. Tarokh, A. Naguib, N. Seshadri, and A. Calderbank, "Space-time codes for high data rate wireless communication: performance criteria in the presence of channel estimation errors, mobility, and multiple paths," *Communications, IEEE Transactions on*, vol. 47, no. 2, Feb. 1999, pp. 199–207.
- [12] T. Schmidl and D. Cox, "Robust frequency and timing synchronization for ofdm," *Communications, IEEE Transactions on*, vol. 45, no. 12, Dec. 1997, pp. 1613–1621.
- [13] A. Rachini, A. Beydoun, F. Nouvel, and B. Beydoun, "Timing synchronization of mimo-ofdm systems," in *LAAS 2014, The 20th International Science Conference*. LAAS, 2014, pp. 149–150.
- [14] U. Rohrs and L. Linde, "Some unique properties and applications of perfect squares minimum phase cazac sequences," in *Communications and Signal Processing, 1992. COMSIG '92., Proceedings of the 1992 South African Symposium on*, Sept. 1992, pp. 155–160.
- [15] B. Yang, K. Letaief, R. Cheng, and Z. Cao, "Burst frame synchronization for ofdm transmission in multipath fading links," in *Vehicular Technology Conference, 1999. VTC 1999 - Fall. IEEE VTS 50th*, vol. 1, 1999, pp. 300–304 vol.1.
- [16] A. Rachini, A. Beydoun, F. Nouvel, and B. Beydoun, "A novel compact preamble structure for timing synchronization in mimo-ofdm systems using cazac sequences," in *INNOV 2013, The Second International Conference on Communications, Computation, Networks and Technologies*, 2013, pp. 1–6.
- [17] J.-J. van de Beek, M. Sandell, M. Isaksson, and P. Ola Borjesson, "Low-complex frame synchronization in ofdm systems," in *Universal Personal Communications. 1995. Record., 1995 Fourth IEEE International Conference on*, Nov. 1995, pp. 982–986.
- [18] L. Li and P. Zhou, "Synchronization for b3g mimo ofdm in dl initial acquisition by cazac sequence," in *Communications, Circuits and Systems Proceedings, 2006 International Conference on*, vol. 2, Jun. 2006, pp. 1035–1039.
- [19] A. Rachini, A. Beydoun, F. Nouvel, and B. Beydoun, "Timing synchronisation method for mimo-ofdm system using orthogonal preamble," in *Telecommunications (ICT), 2012 19th International Conference on*. IEEE, 2012, pp. 1–5.
- [20] A. Rachini, F. Nouvel, A. Beydoun, and B. Beydoun, "A novel timing synchronization method for mimo-ofdm systems," *International Journal On Advances in Telecommunications*, vol. 7, no. 1 and 2, 2014, pp. 22–33.
- [21] R. Frank, S. Zadoff, and R. Heimiller, "Phase shift pulse codes with good periodic correlation properties (corresp.)," *Information Theory, IRE Transactions on*, vol. 8, no. 6, Oct. 1962, pp. 381–382.
- [22] W. Jian, L. Jianguo, and D. Li, "Synchronization for mimo ofdm systems with loosely synchronous (ls) codes," in *Wireless Communications, Networking and Mobile Computing, 2007. WiCom 2007. International Conference on*, Sept. 2007, pp. 254–258.
- [23] G. Gaurshetti and S. Khobragade, "Orthogonal cyclic prefix for time synchronization in mimo-ofdm," *International Journal of Advanced Electrical and Electronics Engineering (IJAEED)*, vol. 2, 2013, pp. 81–85.
- [24] F. Farhan, "Study of timing synchronization in MIMO-OFDM systems using DVB-T," *CoRR*, vol. abs/1404.7843, 2014. [Online]. Available: <http://arxiv.org/abs/1404.7843>
- [25] H.-C. Wang and C.-L. Wang, "A compact preamble design for synchronization in distributed mimo ofdm systems," in *Vehicular Technology Conference (VTC Fall), 2011 IEEE*, Sept. 2011, pp. 1–4.
- [26] R. Gold, "Optimal binary sequences for spread spectrum multiplexing (corresp.)," *Information Theory, IEEE Transactions on*, vol. 13, no. 4, Oct. 1967, pp. 619–621.
- [27] J. G. Proakis, *Digital Communications*, 4th ed. McGraw-Hill, 2000.
- [28] R. Frank, S. Zadoff, and R. Heimiller, "Phase shift pulse codes with good periodic correlation properties (corresp.)," *Information Theory, IRE Transactions on*, vol. 8, no. 6, Oct. 1962, pp. 381–382.
- [29] B. O'Hara and A. Petrick, *The IEEE 802.11 Handbook: A Designer's Companion*. Standards Information Network IEEE Press, 1999.